Int. J. Solids Structures Vol. 23, No. 7, pp. 919–935, 1987
Printed in Great Britain.

0020-7683/87 $3.00+ .00

NON-LINEAR TEMPERATURE–CURVATURE RELATIONSHIPS FOR UNSYMMETRIC GRAPHITE–EPOXY LAMINATES

AKIRA HAMAMOTO
Ishikawajima-Harima Heavy Industries Co., Ltd., Research Institute, Machinery Department, 1, Shin-Nakahara-Cho, Isogo-ku, Yokahama, Japan 235

and

M. W. HYER
Department of Mechanical Engineering, University of Maryland, College Park, MD 20742, U.S.A.

(*Received* 10 *February* 1986)

Abstract—A geometrically non-linear theory is used to study the relationship between temperature and curvature of unsymmetric elevated temperature cure graphite–epoxy laminates. Numerical and experimental results are obtained for square $(0_4/90_4)_T$ laminates of various sizes. It is shown that over a certain temperature range the temperature–curvature relationship of unsymmetric laminates can bifurcate and be triple valued. The triple-valued relationship indicates that more than one laminate shape is possible at a given temperature. Two shapes are cylindrical and the third is a saddle shape. The temperature range over which the relationship is multivalued depends on the size of the laminate. A stability analysis shows that when a multivalued relationship exists, the saddle shape is an unstable equilibrium configuration. When the single-valued saddle shape solution exists, it is a stable equilibrium configuration. Experiments are described which were used to obtain data to compare with the predictions of the theory. Comparisons with experiments are quite good. As might be expected, the sharpness of the theoretical temperature–curvature relationship near the bifurcation points is not realized in the experiments. It is shown how imperfections in the laminate can be included in the theory to account for the more realistic behavior.

INTRODUCTION

Of the wide variety of laminates that can be fabricated using fiber-reinforced material, unsymmetric laminates are rarely made for structural purposes. Like a bimetallic strip, an unsymmetric laminate changes shape with temperature and it exhibits bending–stretching coupling. Unsymmetric laminates are used primarily to determine the stress-free temperature of a material system; or they are used to determine the influence of moisture, radiation, or other environmental factors on material behavior[1–4]. Moisture and radiation, for example, influence the epoxy in graphite–epoxy and unsymmetric laminates can be used to quantify the effects. From the structural viewpoint, the shape change with temperature and the bending–stretching coupling characteristics are usually unwanted and difficult to deal with. On the other hand, it is precisely these characteristics which are used to advantage in material behavior studies. Typically, the curvature of an unsymmetric laminate is measured as a function of an environmental parameter, e.g. temperature or percent moisture absorbed. Using fundamental mechanics and experimental curvature data, inferences are made regarding material behavior, e.g. stress-free temperature or coefficient of moisture expansion. Classical lamination theory usually forms the basis for determining the curvature response of the unsymmetric laminates. Embedded in the theory is the assumption that the linear strain–displacement relations are valid. Specifically, classical lamination theory as presented in Refs [5–8] is used despite the fact that the curvature associated with the response of unsymmetric laminates can cause out of plane deflections that are many times the laminate thickness. Because of these large deflections, the problem is, strictly speaking, geometrically nonlinear. Hence the linear strain–displacement relations are not applicable. Hyer discussed this in a series of papers[9, 10] and explained behavior of unsymmetric laminates that had not been explained before, and in fact, could not be

explained without accounting for geometric nonlinearities. The previous discussions centered on the room-temperature shape of unsymmetric laminates. Specifically, the room-temperature shapes of cross-ply laminates as a function of laminate geometry and stacking sequence were discussed. This paper takes an alternative view of the phenomenon. It examines the shapes of unsymmetrically laminated composites of fixed size as a function of temperature. For the geometrically linear problem the alternative viewpoint would border on being trivial. However, since the problem is nonlinear, new and interesting information evolves from the alternate view.

This paper begins by describing the specific phenomenon being discussed. The geometry and nomenclature used to describe the problem are presented. An overview of the derivation of the governing equations will then be given. Since most of the details of the derivation can be found in previous work, the treatment will be light. Next, theoretical predictions for the shape laminates as a function of temperature are presented. These are new results and they will be discussed in some detail. The experimental procedures used with actual laminates to obtain data for comparison with the theoretical predictions are then discussed. Comparisons between theory and experiment follow. It will be seen that although the comparisons between theory and experiment are reasonable, there are disparities. For this reason the discussion returns to the theoretical shape predictions. This time the effect on laminate shape of slight imperfections in the laminate, e.g. laminate of slightly different thicknesses, are considered. The experimental data are re-examined in light of these modified predictions. The paper ends with several pertinent remarks.

DESCRIPTION OF PROBLEM AND DERIVATION OF THE GOVERNING EQUATIONS

The phenomenon being studied and the geometry used to describe it are summarized in the four portions of Fig. 1. Figure 1(a) shows a square $[0_n/90_n]_T$, $n = 1, 2, \ldots$ laminate at its elevated stress-free temperature. At this temperature the laminate is flat. Figure 1(a) also shows the orientation of the x, y, z-coordinate system used throughout the paper. This paper will consider only square laminates. The 0° direction is aligned with the x-axis and

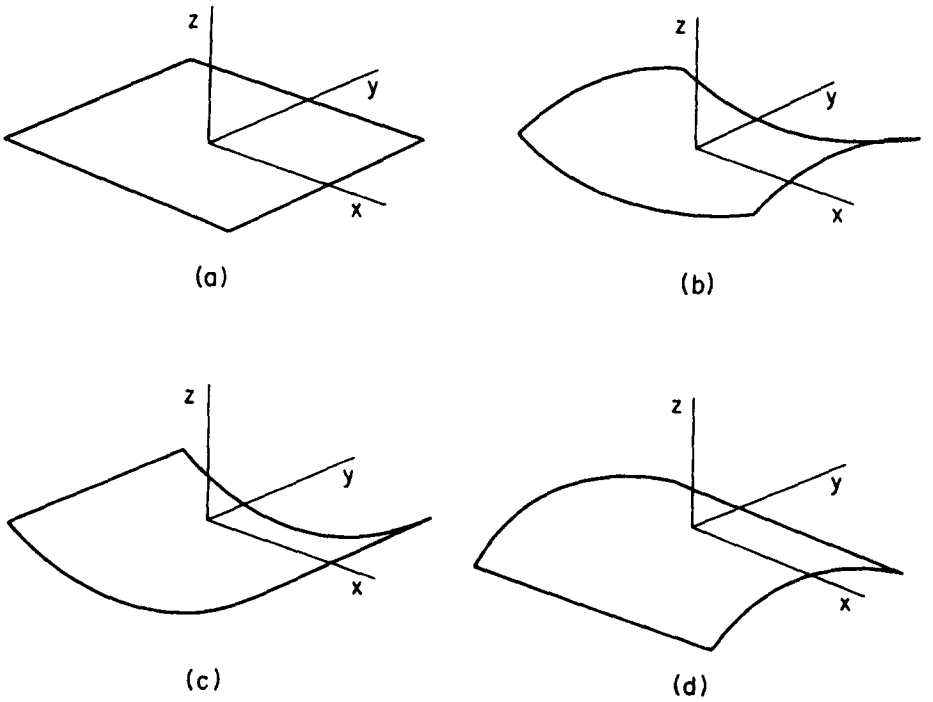

Fig. 1. Laminate shapes: (a) flat at the stress-free temperatures; (b) a saddle; (c) a cylinder; (d) another cylinder.

the leftmost entry in the stacking sequence notation refers to the lamina at the most negative z-position.

As the temperature is reduced from the stress-free condition to room temperature, differences in thermal expansion in the fiber and matrix direction in the different lamina cause the laminate to warp out of plane. (It is assumed here that the temperature is not a function of the spatial coordinates.) Figure 1(b) shows the temperature-induced shape as predicted by classical lamination theory and sometimes observed in practice. It has a saddle shape. (For the cases studied here the saddles will have equal and opposite principal curvatures. This is the result of the particular laminates studied. Equal and opposite curvatures are not "built in" to the theory.) Since the laminate has only 0° or 90° laminate, the principal curvatures will be coincident with the x- and y-axes. Figures 1(c) and (d) show the two cylindrical shapes more frequently observed in practice. In Fig. 1(c) the principal curvature in the y-direction is zero while the x-direction curvature is positive. In Fig. 1(d) the y-direction curvature is negative while the x-direction curvature is zero. (Again, for the cases studied here the magnitudes of the curvatures of the two cylinders in Figs 1(c) and (d) will be equal.) In an actual laminate the shape of Fig. 1(c) can be transformed to the shape of Fig. 1(d) by a simple snap-through action.

The problem here will focus on predicting which shape or shapes the laminate will deform into as it cools from the elevated cure temperature to room temperature in a quasi-static manner. A linear theory predicts only the saddle of Fig. 1(b) can exist. Obviously if the laminates contained laminae with fibers oriented at angles other than 0° or 90°, the scenario of Figs 1(b)–(d) would not be valid and the situation would be much more complex.

The behavior of a laminate will be studied by examining its total potential energy. At a given temperature below cure, the shape (or shapes) which minimize the total potential energy will be the one(s) to occur. Since the problem is nonlinear, the total potential energy is examined within the context of Ritz approximations to the displacement field.

The total potential energy of the laminate, W, including the effects of thermal expansion, is given by

$$W = \int_{\text{Vol}} (\tfrac{1}{2} C_{ijkl} e_{ij} e_{kl} - \beta_{ij} v_{ij} \Delta T)\, \text{dVol} \tag{1}$$

where the standard summation convention on the indices i, j, k, and l is implied and the indices each have values 1, 2, and 3. The C_{ijkl} are the elastic constants of the material and the β_{ij} are constants related to the elastic and thermal expansion properties of the material. The e_{ij} are the strains in the material and ΔT is the temperature change of the material relative to the stress-free temperature. A positive ΔT corresponds to a temperature increase. For simplicity the C_{ijkl} and β_{ij} are assumed to be independent of temperature. With this nomenclature, Hooke's law takes the form

$$\sigma_{ij} = C_{ijkl}(e_{kl} - \alpha_{kl} \Delta T) \tag{2}$$

where α_{kl} are the linear coefficients of thermal expansion. The volume integral is over the undeformed volume of material, Fig. 1(a). The undeformed laminate has dimensions $L_x \times L_y \times h$. (Although results will be for square laminates, $L_x = L_y = L$, the derivation is done for rectangular laminates.) With the origin of the x, y, z-coordinate system at the geometric center of the undeformed volume, the limits on the volume integral are

$$W = \int_{z=-h/2}^{h/2} \int_{y=-L_y/2}^{L_y/2} \int_{x=-L_x/2}^{L_x/2} (\tfrac{1}{2} C_{ijkl} e_{ij} e_{kl} - \beta_{ij} e_{ij} \Delta T)\, dx\, dy\, dz. \tag{3}$$

Since there are no mechanical loads acting on the laminate, there is no contribution to the total potential energy from loads.

If each lamina is assumed to be in a state of plane stress (a valid assumption for thin laminates), then the total potential energy expression simplifies to

$$W = \int_{z=-h/2}^{h/2} \int_{y=-L_y/2}^{L_y/2} \int_{x=-L_x/2}^{L_x/2} (\tfrac{1}{2}\bar{Q}_{11}e_{11}^2 + \bar{Q}_{12}e_{11}e_{22} + 2\bar{Q}_{66}e_{12}^2 + \tfrac{1}{2}\bar{Q}_{22}e_{22}^2 - (\bar{Q}_{11}\alpha_x + \bar{Q}_{12}\alpha_y)e_{11}\Delta T - (\bar{Q}_{12}\alpha_x + \bar{Q}_{22}\alpha_y)e_{22}\Delta T)\, dx\, dy\, dz. \quad (4)$$

The $\bar{Q}_{ij}$'s are the reduced stiffnesses[5–8] of the material and α_x and α_y are the coefficients of thermal expansion of the material in the x- and y-directions, respectively. (Since the work here deals only with cross-ply laminates, $\bar{Q}_{16}$, $\bar{Q}_{26}$, and α_{xy} are identically zero.) Using the usual assumption that the Kirchhoff hypothesis is valid for the laminate as a whole, the strain–displacement relations take the form

$$e_{11} = \varepsilon_x^0 - z\frac{\partial^2 w}{\partial x^2} \quad (5)$$

$$e_{22} = \varepsilon_y^0 - z\frac{\partial^2 w}{\partial y^2} \quad (6)$$

$$e_{12} = \varepsilon_{xy}^0 - z\frac{\partial^2 w}{\partial y\,\partial x} \quad (7)$$

with

$$\varepsilon_x^0 = \frac{\partial u^0}{\partial x} + \frac{1}{2}\left(\frac{\partial w}{\partial x}\right)^2 \quad (8)$$

$$\varepsilon_y^0 = \frac{\partial v^0}{\partial y} + \frac{1}{2}\left(\frac{\partial w}{\partial y}\right)^2 \quad (9)$$

$$\varepsilon_{xy}^0 = \frac{1}{2}\left(\frac{\partial u^0}{\partial y} + \frac{\partial v^0}{\partial x} + \frac{\partial w}{\partial x}\frac{\partial w}{\partial y}\right). \quad (10)$$

The quantities u^0, v^0, and w are the displacements of the laminate midplane in the x-, y- and z-directions, respectively. They are functions of x and y only. The terms ε_x^0, ε_y^0, and ε_{xy}^0 are called the midplane strains and the form given for them in eqns (8)–(10) reflect inclusion of non-linear effects.

The displacements can be approximated by the functional forms

$$u^0(x,y) = cx - \frac{a^2x^3}{6} - \frac{abxy^2}{4} \quad (11)$$

$$v^0(x,y) = dy - \frac{b^2y^3}{6} - \frac{abx^2y}{4} \quad (12)$$

$$w(x,y) = \tfrac{1}{2}(ax^2 + by^2). \quad (13)$$

In the above a, b, c, and d are constants which are determined as part of the minimization process. Constants a and b are directly related to the out-of-plane shape of the deformed laminate, $a = -b$ representing a perfect saddle (Fig. 1(b)), $a > 0$, $b = 0$ representing a cylinder (Fig. 1(c)), and $a = 0$, $b < 0$ representing another cylinder (Fig. 1(d)). Constants a and b are approximations to the x- and y-direction curvatures, respectively, and will be used here as a measure of laminate shape. Constants c and d represent inplane strains. The above functional forms were motivated by the following:

(1) eqn (13) is a good approximation to the situation depicted in Fig. 1;

(2) a significant portion of the u^0 and v^0 displacements are due to the laminate curling into a cylinder or saddle, and;

(3) the midplane shear strains, ε^0_{xy}, in a cross-ply laminate are insignificant and can be assumed to be zero.

Equations (11)–(13) are substituted into eqns (5)–(10) and these in turn into eqn (4) to give W as a function of a, b, c, and d... as well as the laminate materials properties, laminate geometry, and temperature change. The integration with respect to x, y, and z is done explicitly. Taking the first variation of W with respect to a, b, c, and d, and setting the variation to zero leads to an equation of the form

$$\delta W = f_1(a,b,c,d)\,\delta a + f_2(a,b,c,d)\,\delta b + f_3(a,b,c,d)\,\delta c + f_4(a,b,c,d)\,\delta d = 0. \quad (14)$$

In particular, this leads to four coupled non-linear algebraic equations for a, b, c, and d, namely

$$f_i(a,b,c,d) = 0, \qquad i = 1,4. \quad (15)$$

Going one step further than the previous work[9, 10], the four equations represented by eqn (15) can be reduced to a single equation in either a or b. These equations are

$$(S^2U_1)a^5 + (S^2V_1)a^4 + (2SU_1U_2)a^3 + (STV_2 + 2SU_2V_1)a^2 + (SV_2^2 - T_2U_2 + U_1U_2^2)a + (U_2^2V_1 - TU_2V_2) = 0 \quad (16a)$$

and

$$b = -\frac{Ta + V_2}{Sa^2 + U_2}; \quad (16b)$$

or

$$(S^2U_2)b^5 + (S^2V_2)b^4 + (2SU_1U_2)b^3 + (STV_1 + 2SU_1V_2)b^2 + (SV_1^2 - T^2U_1 + U_1^2U_2)b + (U_1^2V_2 - TU_1V_1) = 0 \quad (17a)$$

and

$$a = -\frac{Tb + V_1}{Sb^2 + U_1}. \quad (17b)$$

The constants are defined as

$$\begin{aligned}
S &= (A_{11}L_y^4 + A_{22}L_x^4)/2880 \\
T &= D_{12} + A_{12}B_{11}B_{22}/(A_{11}A_{22} - A_{12}^2) \\
U &= D_{11} - A_{22}B_{11}^2/(A_{11}A_{22} - A_{12}^2) \\
U_2 &= D_{22} - A_{11}B_{22}^2/(A_{11}A_{22} - A_{12}^2) \\
V_1 &= M_x^T - B_{11}(A_{22}N_x^T - A_{12}N_y^T)/(A_{11}A_{22} - A_{12}^2) \\
V_2 &= M_y^T - B_{22}(A_{11}N_y^T - A_{12}N_x^T)/(A_{11}A_{22} - A_{12}^2).
\end{aligned} \quad (18)$$

The A_{ij}, B_{ij}, and D_{ij} have the usual definitions associated with laminates[5–8]. The quantities N_x^T, N_y^T, M_x^T, and M_y^T are the effective inplane thermal loads and the effective thermal moments, respectively. They are defined by

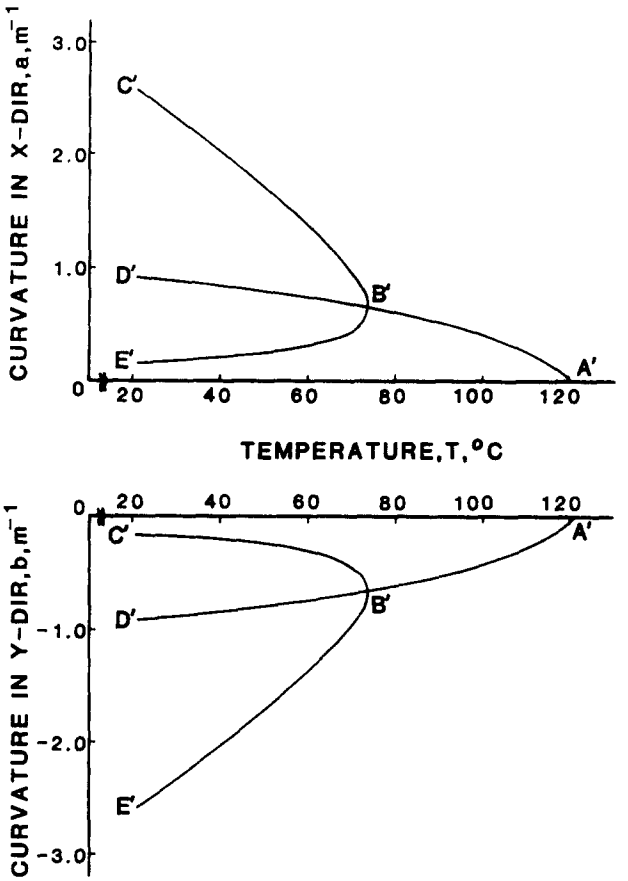

Fig. 2. Temperature–curvature relation of a 125 × 125 mm $(0_4/90_4)_T$ AS4/1908 graphite–epoxy laminate.

$$
\begin{aligned}
N_x^T &= \Delta T \int_{-h/2}^{h/2} (\bar{Q}_{11}\alpha_x + \bar{Q}_{12}\alpha_y)\, dz \\
N_y^T &= \Delta T \int_{-h/2}^{h/2} (\bar{Q}_{12}\alpha_x + \bar{Q}_{22}\alpha_y)\, dz \\
M_x^T &= \Delta T \int_{-h/2}^{h/2} (\bar{Q}_{11}\alpha_x + \bar{Q}_{12}\alpha_y) z\, dz \\
M_y^T &= \Delta T \int_{-h/2}^{h/2} (\bar{Q}_{12}\alpha_x + \bar{Q}_{22}\alpha_y) z\, dz.
\end{aligned} \tag{19}
$$

The stability of the various equilibrium configurations can be determined by examining higher-order variations of W with respect to a, b, c, and d. With this system the second variation generally did not vanish and could be used for stability analysis. However, the bifurcation points were not checked. From past experience, higher-order variations involving considerably more algebra would govern the stability at those points and, in addition, it is impossible to construct a laminate that is governed by those points. Therefore, the analytical effort stopped short of a complete stability analysis.

The next section presents predictions for the shapes of laminates as a function of temperature, as well as size. The results are based on solving the single non-linear equation, eqn (16a), and a stability analysis.

NUMERICAL RESULTS

Figure 2 illustrates the relationship between the temperature and the curvature of a 125 × 125 mm $(0_4/90_4)_T$ laminate fabricated from AS4/1908 graphite–epoxy. Temperatures

from the stress-free temperature down to room temperature are considered. The upper portion of the figure shows the relationship between the x-direction curvature, a, and the temperature. The lower portion of the figure shows the relation between the y-direction curvature, b, and temperature. There are multiple solutions to both these relations and these solution branches are annotated with the letters A′, B′, C′, D′, and E′. AS4/1908 is manufactured by Hercules, Inc.† and has a curing temperature of 121°C. For this material the stress-free temperature is close to the curing temperature. Room temperature was assumed to be 20°C. The material properties used in obtaining numerical results for the AS4/1908 laminates were

$$E_1 = 115 \text{ GPa}$$
$$E_2 = 8 \text{ GPa}$$
$$\nu_{12} = 0.28$$
$$\alpha_1 - \alpha_2 = -48 \times 10^{-6} °\text{C}^{-1}$$
$$\text{lamina thickness} = 0.175 \text{ mm}.$$

Several features of the relationship between laminate curvatures and laminate temperature are immediately obvious from the figure. First, there is a symmetry to the relationship between the two curvatures and the temperatures. The upper and lower portions of the figure are mirror images of each other. Second, over a certain range of temperatures the temperature–curvature relation is single valued while over another range the relation is triple valued. These and other features of the relation will now be discussed and interpreted.

Referring to Fig. 2, point A′ corresponds to the situation shown in Fig. 1(a), namely the laminate in the flat stress-free state. As the temperature is reduced, curvatures develop in the laminate. Though small at first, the curvatures are equal and opposite and so the laminate is saddle shaped. As the temperature is reduced more, the saddle becomes deeper and deeper. At a temperature corresponding to point B′, the temperature–curvature relation bifurcates. A further reduction of temperature results in the laminate following one of three possible temperature–curvature paths. If the laminate follows path B′C′, then the curvature in the x-direction continues to increase while the curvature in the y-direction decreases. Alternatively, if the laminate follows path B′E′, then the curvature in the y-direction continues to increase, in magnitude, and the curvature in the x-direction decreases. As a third possibility, if the laminate follows path B′D′ as it cools, then it will remain a saddle with equal and opposite curvatures, the saddle becoming deeper as the temperature is lowered.

Figure 3 shows the temperature–curvature relationship for a 300×300 mm $(0_4/90_4)_T$ AS4/1908 graphite–epoxy laminate. The format of the axes is the same as in the previous figure. The temperature–shape characteristics of this laminate are similar to the characteristics of the 125×125 mm laminates. For this larger laminate, however, the differences in the shapes represented by the different solution branches are more distinct than they are for the 125×125 mm laminate. As the temperature is lowered from the stress-free temperature, equal and opposite curvatures develop. At less than 10°C below the stress-free temperature, the solution bifurcates. If as the temperature is reduced further the laminate follows path B′C′, then the x-direction curvature continues to increase while the y-direction curvature virtually disappears. This corresponds to the cylindrical shape of Fig. 1(c). Alternatively, if the cooling path follows path B′E′, then the y-direction curvature increases in magnitude and the x-direction curvature disappears. This corresponds to the cylindrical shape of Fig. 1(d). Path B′D′ represents a laminate with equal and opposite curvature, a saddle. For the 125×125 mm laminate the shapes represented by branches B′C′ and B′E′ are not quite cylindrical. The tendency is there but the effect is not as pronounced as it is with the 300×300 mm laminate.

A stability analysis indicates that solutions on branches B′C′ and B′E′ are stable. However, solutions on saddle branch B′D′ are unstable. These findings are important. They

† Hercules, Inc., Magna, UT 84044, U.S.A.

indicate that as the laminate is cooled, at temperatures below the bifurcation temperature a laminate with equal and opposite curvatures will never be observed. Instead, for the 300 × 300 mm laminate either of two cylindrical equilibrium configurations will be observed. Since either of two equilibrium configurations are possible, the laminate can be changed from one configuration to the other by application of an external force. This is commonly done at room temperature and when it is done the laminate changes from one configuration to the other with an audible snap.

Figure 4 illustrates the temperature–curvature relationship for a 50 × 50 mm $(0_4/90_4)_T$ laminate, one smaller than either of the two just considered. The temperature–curvature relation for this smaller laminate is markedly different than the two previous ones. The important differences are the lack of any bifurcation temperature and the fact that the laminate will remain a saddle over the entire temperature range. This single solution is stable and, compared to the linear relation predicted by the classical theory (results not shown) is slightly nonlinear.

EXPERIMENTAL PROCEDURE FOR MEASURING TEMPERATURE–CURVATURE RELATIONS

To empirically study the temperature–curvature relations of unsymmetric laminates, experiments were conducted using two graphite–epoxy materials. The materials were the AS4/1908 material, used in the calculations above, and AS4/3502. The AS4/3502 material has a cure temperature of 177°C and a stress-free temperature above that. It is also manufactured by Hercules, Inc. Experimental as well as numerical results were obtained for AS4/3502 mainly to determine the effects of different stress-free temperatures on the temperature–curvature relations. The curvature measurements were made with strain gages, during heating and cooling, and a dial gage and a movable horizontal table when the laminates were at room temperature. Temperature measurements were made with standard

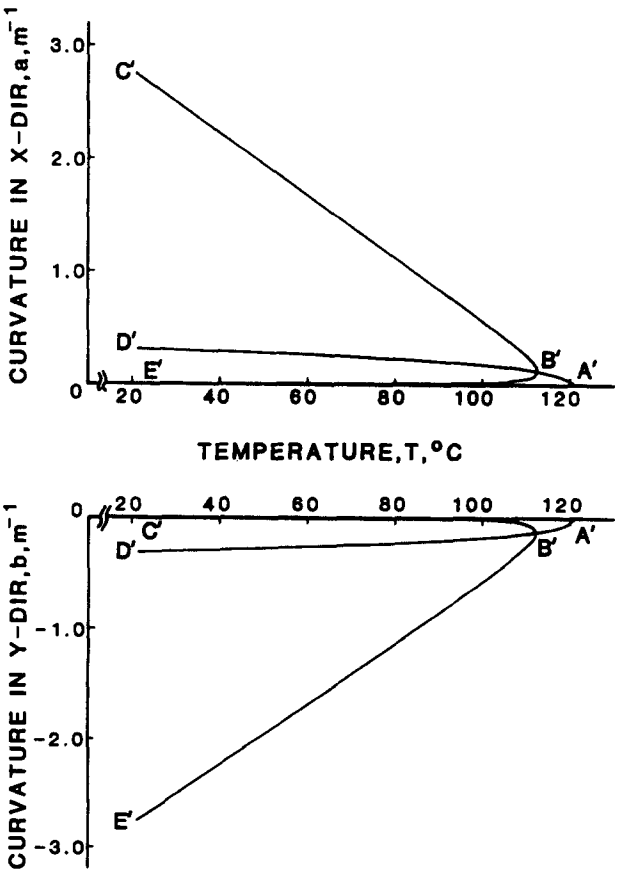

Fig. 3. Temperature–curvature relation of a 300 × 300 mm $(0_4/90_4)_T$ AS4/1908 graphite–epoxy laminate.

thermocouples. With the laminate mounted on it, the table and dial gage could be used to measure the out-of-plane deformation of the laminate as a function of x and y.

A 300×300 mm $(0_4/90_4)_T$ AS4/1908 laminate was fabricated in an autoclave in accordance with the instructions from Hercules. Upon removal from the autoclave the laminate was cylindrical, the shape which was expected in the light of the predictions of Fig. 3. From measurements it was clear that the laminate was not of uniform thickness, the laminate being thicker in the center than it was along the edges. The nominal thickness was 1.40 mm and this varied by 0.08 mm from the center to the outer edges. After measuring the laminate thickness the laminate was heated to 70–80°C for about 3 days to dry it. The laminate was then thermally cycled several times from room temperature to just below the cure temperature to effect a post-cure. The post-cure was important because the laminate needed to be stable (chemically) and free of any chemical shrinkage during the heating and cooling when curvatures were being measured as a function of temperature.

After drying and post-curing, strain gages were mounted near the center of the laminate. Back-to-back gages in both the x- and y-directions were used. After mounting the strain gages the room-temperature curvature of the laminate was determined by using the table-dial gage set-up. The laminate was then placed in a circulating hot air oven, the temperature of the oven was slowly increased, and temperature and strain data recorded roughly every 10°C. When the temperature reached the desired maximum, the temperature was slowly reduced. This was repeated for several cycles. The temperature changes were controlled by hand and the heating and cooling rates never exceeded 25°C h^{-1}. Using the bending strain data and the measured laminate thickness, the change in curvature relative to the room-temperature curvature was computed and tabulated as a function of temperature.

After the measurements were made on the 300×300 mm laminate, its size was reduced to 125×125 mm by cutting. By making the smaller laminate from the larger one, material

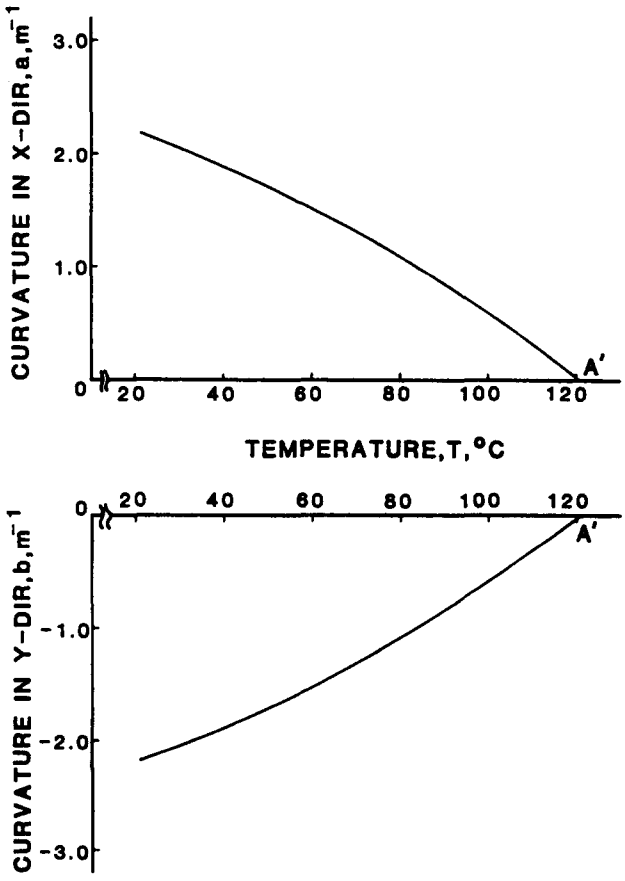

Fig. 4. Temperature–curvature relation of a 50×50 mm $(0_4/90_4)_T$ AS4/1908 graphite–epoxy laminate.

variability issues would be minimized and, in fact, eliminated. Cutting was done with the strain gages in place and the same gages and gage installations were reused, further reducing variability. With care in cutting, the strain gage installation was not disturbed. Similar heating and cooling measurements were then made on the smaller laminate, after its room-temperature shape had been measured. The same procedures were also followed for the laminate made from AS4/3502 but only a 150 x 150 mm laminate was studied. Therefore, no cutting was involved.

To have a good estimate of the material properties of the particular laminates being tested, to use in making theoretical predictions, measurements directly from the laminates, some Hercules data, and thermal expansion measurements from $(0)_8$ laminates were used. By measuring the specific gravity of small pieces of the laminates and knowing the density of the epoxy and the graphite-fibers, the volume fraction of the composite was estimated. Using known fiber and epoxy moduli, the moduli of an individual lamina was estimated. Thickness measurements of the laminates were used to estimate the thickness of an individual lamina. Strain gages mounted on a $(0)_8$ laminate were used to measure the lamina thermal expansion coefficients, α_1 and α_2, over the temperature range of interest. The theory required only the knowledge of the difference in the lamina thermal expansion coefficients, $\alpha_1 - \alpha_2$. For all intents and purposes, the difference in expansion coefficients was constant over the temperature range to be studied. During these expansion measurements it was found that three or four thermal cycles were enough to effect a post-cure of the material. After three or four cycles the thermal expansion measurements were repeated and found to be consistent. Before that number of cycles, the thermal expansion vs temperature relations exhibited what could be interpreted as hysteresis.

When not being used for some portion of the experiments, the laminate was stored in a desiccator.

COMPARISON OF THEORY AND EXPERIMENT: AS4/1908

Figure 5 shows a comparison between the theoretical predictions of the previous section and experimental results for one heating and cooling cycle the 125 mm square AS4/1908 $(0_4/90_4)_T$ laminate. The temperature of the laminate began at room temperature, was increased to about 120°C, and then was decreased to room temperature again. The open circles in the figure represent the measurements taken while heating. The crosses represent cooling data. As can be seen, as the temperature was increased from room temperature, the x-direction curvature decreased, closely following the theoretical prediction until near the bifurcation temperature. After the bifurcation temperature the experimental results did not follow the predicted temperature–curvature relation as closely as at the lower temperatures. The theoretical temperature–curvature relation predicted a sharp inflection at the bifurcation temperature. The experimental data did not show the sharp inflection. The x-direction curvature went to zero very close to the predicted temperature.

The y-direction curvature generally behaved as predicted. At the lower temperatures the quantitative comparisons were not as good as the qualitative comparisons. At the bifurcation temperature the quantitative comparison began to improve and from the bifurcation temperature to the stress-free temperature, the comparison between theory and experiment was good. Again the sharpness of the inflection was missing in the experimental data. The y-direction curvature disappeared at the predicted temperature.

The cooling paths for both curvatures very closely retraced the heating path. As might be expected in light of the previous discussions, the relation between the heating and cooling path would be strongly affected by whether or not the laminate was dry when the experiment began, and whether or not the laminate was post-cured prior to the experimental phase. A laminate which contains absorbed moisture (typical maximum values of absorbed moisture being 1–3% of the laminate weight) dries out as it is heated. Since moisture within the laminate swells the laminate much like a thermal expansion effect, the drying out of the laminate by heating causes a shrinkage within the laminate. Upon cooling, the laminate is drier and the temperature–curvature path is different than the heating path. Moisture

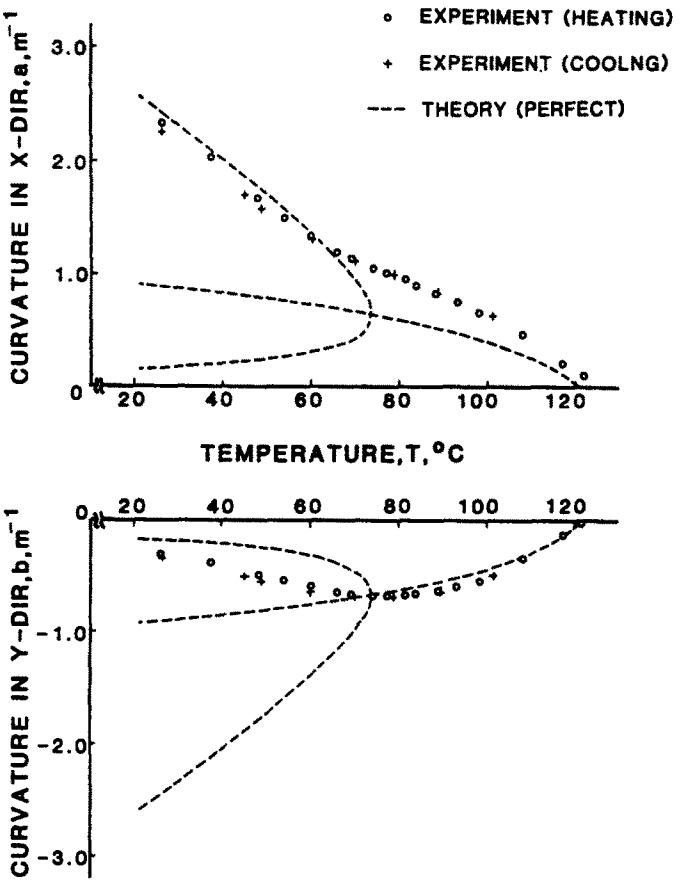

Fig. 5. Comparison between theory and experiment for the 125 × 125 mm $(0_4/90_4)_T$ AS4/1908 graphite–epoxy laminate.

swelling effects can be accounted for but it is easier to work with dry laminates, as was done here. Failing to satisfactorily post-cure the laminate would result in similar heating and cooling path differences.

Figure 6 shows a comparison between theory and experiment for a 300 mm square AS4/1908 $(0_4/90_4)_T$ laminate. As the laminate was heated the measured temperature–curvature relation was quite close to the predicted results for both curvatures. At the lower temperature the y-direction curvature was predicted to be effectively non-existent. The experimental measurements confirm this. Near the bifurcation temperature the y-direction curvature was predicted to be slightly negative. The experimental data confirmed this also. However, near the bifurcation temperature the x-direction curvature again did not follow the predicted sharp inflection. Data were taken at small temperature intervals near the bifurcation temperature to be sure to follow the inflection. However, at the bifurcation temperature the curvatures were so close to zero that small errors in the measurements could effect whether or not the data appeared to follow the inflection in the relation in this region. The data did not appear to follow the predicted relation but the curvatures did disappear very close to the predicted temperature. The cooling portion of the cycle followed very closely the heating portion of the cycle.

The experimental data, though not exhibiting 100% correlation with the predicted results, did show that a theory which includes geometric nonlinearities is necessary to predict the phenomenon. The empirically determined temperature–curvature relation for each curvature was not linear and the y-direction curvature was not equal in magnitude to the x-direction curvature. A geometrically linear theory is simply not valid. However, the non-linear theory as presented still did not seem to predict the behavior of the laminates near the bifurcation temperature. This is discussed next.

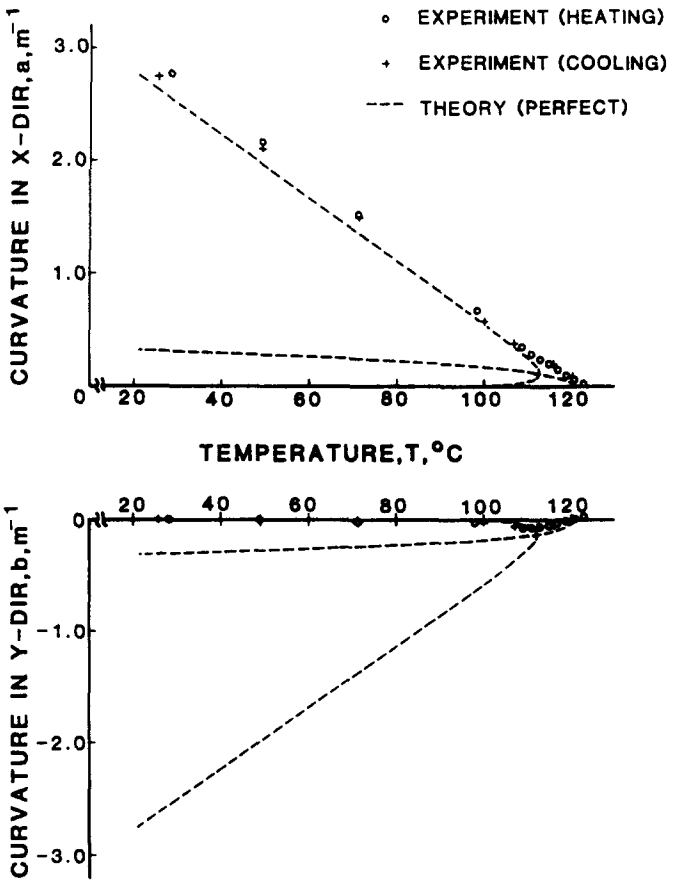

Fig. 6. Comparison between theory and experiment for the 300 × 300 mm $(0_4/90_4)_T$ AS4/1908 graphite–epoxy laminate.

THE EFFECT OF IMPERFECTIONS ON THE PREDICTED RESPONSE

The theory presented so far represented what could be considered the ideal or perfect $(0_4/90_4)_T$ laminate. It was assumed that the material properties were uniform with spatial position within the laminate, that each lamina was identical, that the thickness of each lamina was uniform, and that the angles of the laminae were exactly 0° or 90°. These assumptions, along with the kinematic assumption incorporated in the formulation of the theory, led to the bifurcation behavior, a behavior that is rarely, if ever, observed in real systems. With fiber-reinforced composite materials there are many problems that could lead to deviations from the ideal and thus represent imperfections. Each lamina comes from a different position on the prepreg tape and so there could well be a slight variation in material properties from one lamina to the next. Also, when fabricating the laminate it is not possible to orient the laminae precisely. Thus a $(0_4/90_4)_T$ laminate could unknowingly be a $(1/0/-0.5/-1/89/90/90.5/91)_T$ laminate because of this limitation. Even if extreme care is taken when orienting each lamina, curved, twisted, and misaligned fibers in the prepreg lead to local variations in the fiber orientation. In addition, when curing the laminate, temperature gradients can lead to non-uniform curing of the laminate. This non-uniform curing leads to non-uniform material properties and differences in epoxy flow from point to point as the material cures. Non-uniform epoxy flow results in differences in fiber volume fraction from one location to the next in the laminate and to variations in thickness of the laminate. As mentioned earlier, thickness variations were measured in all laminates tested. These variations were felt to be directly related to the curing process.

Because of these limitations with achieving the ideal, it is logical to ask what effect imperfections have on the predicted response. Unfortunately, the theory developed is limited to laminates with lamina that are orthotropic in the x, y, z-system. This translates into considering only 0° or 90° lamina. Also, each lamina must have spatially uniform material

properties and thickness. Therefore, the theory could not be used to measure the effect of certain types of imperfections. However, the material properties of each lamina could be made to differ slightly and the thickness of each lamina could be slightly different. Figure 7 shows the effect of a slightly different lamina thickness on the temperature–curvature relation of the $(0_4/90_4)_T$ AS4/1908 discussed in Fig. 2. In Fig. 7 the results of Fig. 2 are repeated and are indicated with a dashed line. The solid line shows the effect of assuming the 0° lamina are 1% thicker and the 90° are 1% thinner than the nominal 0.175 mm quoted earlier. As can be seen, this slight imperfection causes the bifurcation behavior to disappear and greatly reduces the sharpness of the temperature–curvature relation near the bifurcation point. The behavior exhibited by the imperfect case is referred to limit point behavior. Limit point behavior is common in real systems and results in disjoint equilibrium paths, as opposed to a bifurcating path. In Fig. 7 point B′ defines the limit point.

While the thickness variation can be used to explain the loss of a distinct and sharp bifurcation, there is no reason to suspect that it is only the thickness variation that caused the loss witnessed here. In fact, there is no reason to suspect that it is exactly this level of imperfection that is present. A slight variation in material properties from lamina to lamina can be made to show the same effect, qualitatively and quantitatively. The purpose of looking at any imperfection at all is to determine the influence of imperfections, in general, on the temperature–curvature relation. It is clear, however, that an imperfection of the type and level depicted in Fig. 7 could very well be responsible for the lack of good correlation between theory and experiment over the entire temperature range, particularly near the bifurcation temperature.

With this idea in mind, Fig. 8 shows a comparison between the data and the theoretical predictions for the 125 mm square laminate. The thickness imperfection discussed above is

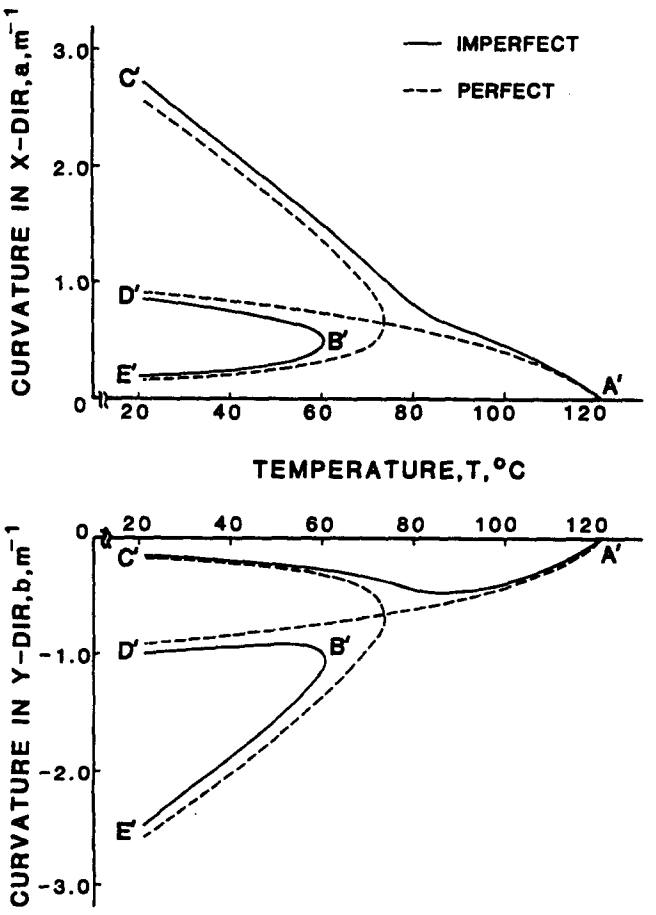

Fig. 7. Effect of a thickness imperfection on the temperature–curvature relation of a 125 × 125 mm $(0_4/90_4)_T$ AS4/1908 graphite–epoxy laminate.

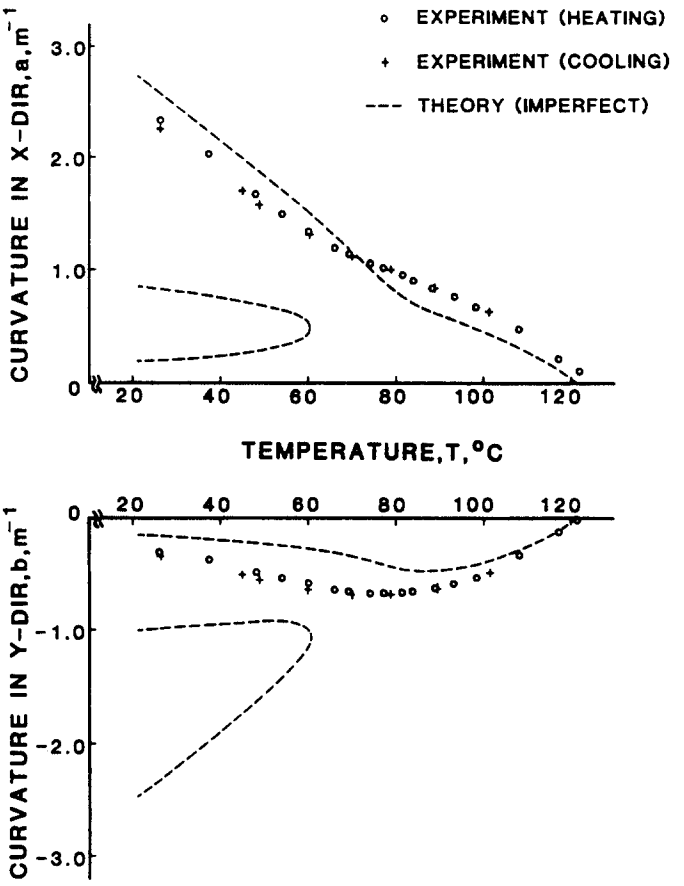

Fig. 8. Comparison between theory and experiment for the 125 × 125 mm $(0_4/90_4)_T$ AS4/1908 graphite–epoxy laminate, thickness imperfection included.

included in the theoretical results. This figure is a combination of the data from Fig. 5 and the imperfect theory from Fig. 7. While the correlation is still not in the very good category, the less sharp inflection in the data and in the theory compare well.

COMPARISON BETWEEN EXPERIMENT AND THEORY: AS4/3502

Figures 9 and 10 show theoretical predictions and experimental data for a 150 mm square $(0_4/90_4)_T$ AS4/3502 laminate. The material properties used to obtain the theoretical results for the material were

$$E_1 = 150 \text{ GPa}$$
$$E_2 = 10 \text{ GPa}$$
$$\nu_{12} = 0.28$$
$$\alpha_1 - \alpha_2 = -29 \times 10^{-6} \,^\circ\text{C}^{-1}$$
$$\text{lamina thickness} = 0.125 \text{ mm}.$$

Unfortunately, in the actual laminate there was what could be considered a significant thickness variation. From the center to the outside edges there was a variation of 0.18 mm, more than one lamina thickness. This translates into a large variation in fiber volume fraction from location to location in the panel. The nominal fiber volume fraction was calculated to be 62%. Therefore, the material property data are best estimates based on engineering judgment.

Despite the problems with thickness variations in this laminate, the data from the laminate shown in the two figures is quite interesting and there is a point to be made. Figure 9 shows the heating and cooling data, and the theory, for the laminate with the preheating

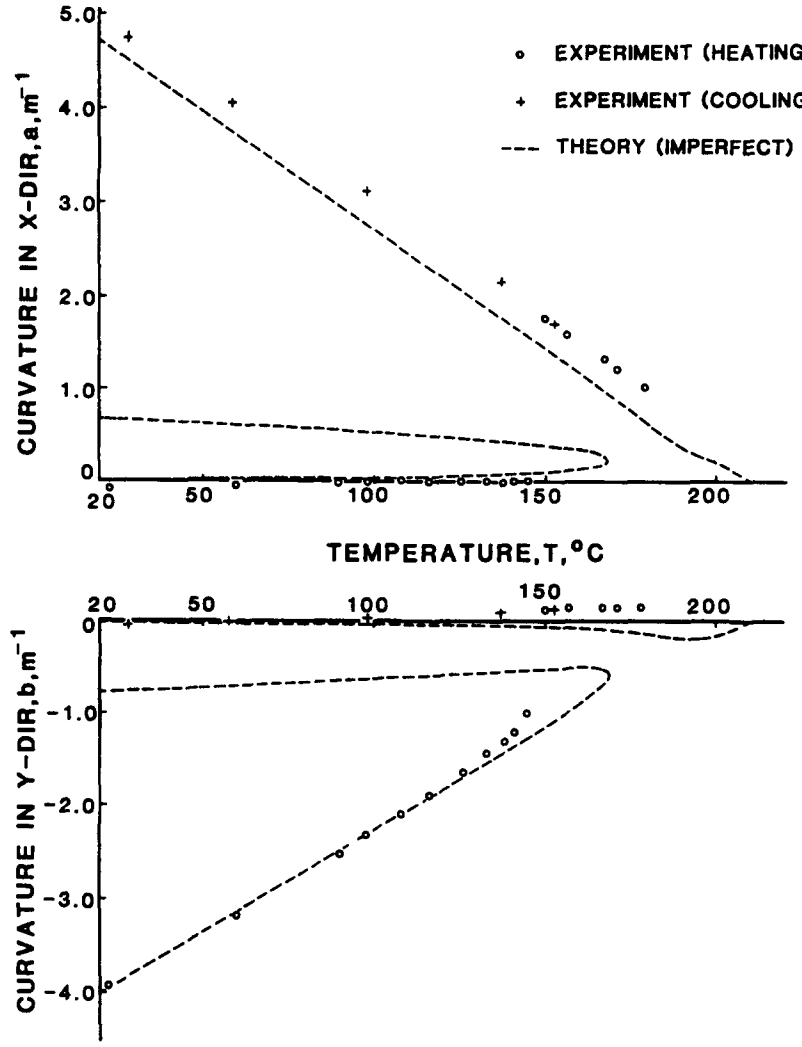

Fig. 9. Comparison between theory and experiment for a 150 × 150 mm $(0_4/90_4)_T$ AS4/3502 graphite–epoxy laminate, thickness imperfection included.

room-temperature x- and y-curvatures as shown in Fig. 1(d). The imperfection in the laminate, in the theoretical calculations, is the form of a thickness imperfection, the 0° lamina being 2% thicker than the nominal value and the 90° lamina being 2% thinner. Initially the y-direction curvature is the primary curvature and there is very little curvature in the x-direction. As the temperature was increased, the magnitude of the y-direction curvature decreased while the curvature in the x-direction remained zero, both behaving as predicted. At about 148°C the shape of the laminate suddenly changed, the y-direction curvature suddenly jumping to zero (or slightly negative, according to the data) and the x-direction curvature suddenly becoming nonzero. As the temperature was increased further the newly-formed x-direction curvature decreased and the y-direction curvature remained zero. At 177°C the temperature was decreased. Upon cooling the y-direction curvature remained zero while the x-direction curvature increased. At room temperature the laminate appeared as in Fig. 1(c). The laminate jumped from one cylindrical configuration to the other during the heating phase because the total potential energy of the second configuration was lower than the energy state of the first configuration. At 148°C the energies were closed enough so that the imperfections in the laminate forced the laminate into the second configuration. Once in that configuration, it stayed there for the remainder of the heating and cooling cycle. In a perfect laminate the energies of the two cylindrical configurations are identical. With an imperfect laminate this is not the case.

Figure 10 shows the heating and cooling paths for the same laminate but with the laminate starting in the configuration it ended in from the cycle of Fig. 9, i.e. the configuration of Fig. 1(c). With the laminate starting in this configuration, the heating and cooling paths are virtually identical. The x-direction curvature goes to zero very close to the temperature predicted and a careful inspection of the upper portion of the figure reveals a slight inflection in both the heating and cooling data near 190°C. This slight inflection is predicted. The point to be noted is that during this heating–cooling cycle the laminate did not jump from one cylindrical shape to the other. Another point to be noted is that the temperature–curvature relation of the 150 × 150 mm AS4/3502 laminate was more like the relation of the 300 × 300 mm AS4/1908 laminate than the relation of the 125 × 125 mm AS4/1908 laminate. Apparently the magnitude of the temperature change below the stress-free temperature is a strong factor in determining whether the temperature–curvature relation shows distinct cylinders or whether there is just the tendency, as was the case with the 125 × 125 mm AS4/1908 laminate.

CONCLUDING COMMENTS

From the results shown, it is clear that unsymmetric laminates exhibit interesting nonlinear effects. Multiple equilibrium configurations and instabilities characterize both the theoretical predictions and the actual laminates. Imperfections seem to control the exact details of the behavior. Before closing, the discussion of several other interesting features are in order.

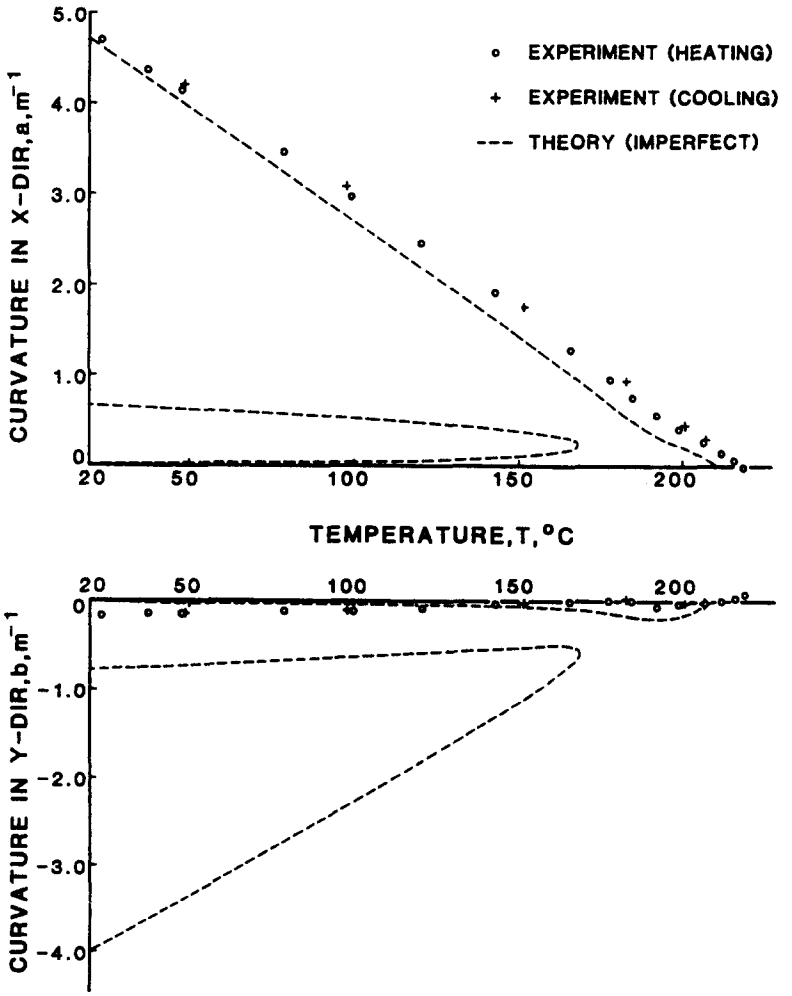

Fig. 10. Comparison between theory and experiment for a 150 × 150 mm $(0_4/90_4)_T$ AS4/3502 graphite–epoxy laminate with another initial shape, thickness imperfection included.

First, there is a simple relationship between the curvature predicted by the linear theory and the curvature of large cylindrical laminates. The predictions of the linear theory can be obtained by letting L_x and $L_y \to 0$ in eqn (16). The result is

$$a = -b = \frac{V_1}{T-U_1} = \frac{24}{h}\frac{(Q_{11}Q_{22}-Q_{12}^2)(\alpha_1-\alpha_2)\Delta T}{Q_{11}^2+14Q_{11}Q_{22}+Q_{22}^2-16Q_{12}^2} \tag{20}$$

where h, recall, is the laminate thickness and the Q_{ij}'s are the stiffness[5–8] of the lamina in the principal material coordinates. For large laminates, letting L_x and $L_y \to \infty$, eqn (16) gives

$$a = -\frac{V_1}{U_1} = \left\{\frac{24}{h}\frac{(Q_{11}Q_{22}-Q_{12}^2)(\alpha_1-\alpha_2)\Delta T}{Q_{11}^2+14Q_{11}Q_{22}+Q_{22}^2-16Q_{12}^2}\right\}\left\{\frac{Q_{11}+Q_{22}-2Q_{12}}{Q_{11}+Q_{22}}\right\}. \tag{21}$$

As can be seen, the limiting curvature for the large laminates is related to the linear prediction. The first bracketed term in eqn (21) is the linear prediction of eqn (20). For both AS4/1908 and AS4/3502 the second bracketed term is equal to 0.96. In both cases the limiting value of the non-zero curvature of the cylindrical laminate is practically identical to the linear prediction. Of course, in the linear theory the other curvature is equal and opposite in sign. In the non-linear theory the other curvature is zero. The closeness of the limiting case of large laminates to the linear theory is forgiving. Material behavior studies, e.g. stress-free temperature or moisture absorption studies, using large laminates but the linear theory will be close to being correct. (Assuming, of course, the behavior of the other curvature is ignored.) In a similar vein, small laminates are also forgiving. The temperature–curvature relation of Fig. 4 is almost linear and neither curvature is zero. This raises the second important point.

For intermediate sized laminates, e.g. the 125 mm square case of Figs 2 and 5, the linear theory predicts that points A′ and C′ of Fig. 2 are connected by a straight line. The perfect theory, the imperfect theory, and experimental data all show this is not the case. For the investigator using data similar to that shown in Fig. 5, the inflection in the data and the behavior of the y-direction curvature would have to be ignored if a linear theory was being used. It is suspected that in much of the reported data this is the case. The x-direction data could be used by considering only the endpoints, i.e. the stress-free temperature and room temperature, or by forcing a straight line through the data. Assuming the y-direction curvature is ignored, there could be reasonable correlation with the linear theory.

REFERENCES

1. N. J. Pagano and H. T. Hahn, Evaluations of composite curing stresses, *Composite Materials: Testing and Design, 4th Conference*, ASTM STP 617, pp. 317–329 (1977).
2. C. T. Herakovich, J. G. Davis, Jr. and J. S. Mills, Thermal microcracking in Celion 6000/PMR-15 graphite-polyimide. In *Thermal Stress in Severe Environment* (Edited by D. P. H. Hasselman and R. A. Heller), pp. 649–664. Plenum, New York (1980).
3. F. W. Crossman, R. E. Mauri and W. J. Warren, Moisture-altered viscoelastic responses of graphite-epoxy composites. In *Advanced Composite Materials—Environmental Effects*, ASTM STP 658, pp. 205–220 (1978).
4. B. D. Harper and Y. Weitsman, Environmental effects in cross-ply composites. *Int. J. Solids Structures* **21**, 907–926 (1985).
5. R. M. Jones, *Mechanics of Composite Materials*. Scripta (available from McGraw-Hill), New York (1975).
6. S. W. Tsai and H. T. Hahn, *Introduction to Composite Materials*. Technomic, Westport, CT 06880 (1980).
7. B. D. Agarwarl and L. J. Broutman, *Analysis and Performance of Fiber Composites*. Wiley, New York (1980).
8. J. M. Whitney, I. M. Daniel and R. B. Pipes, *Experimental Mechanics of Fiber Reinforced Composite Materials*. Society of Experimental Mechanics, 14 Fairfield Drive, Brookfield Center, CT 06805 (1982).
9. M. W. Hyer, Calculations of the room-temperature shapes of unsymmetric laminates. *J. Composite Materials* **15**, 296–310 (1981).
10. M. W. Hyer, The room-temperature shapes of four-layer unsymmetric cross-ply laminates. *J. Composite Materials* **16**, 318–340 (1982).